Metals **2011**, *1*, 65-78; doi:10.3390/met1010065

OPEN ACCESS

metals

ISSN 2075-4701

www.mdpi.com/journal/metals/

Article

Particle Based Alloying by Accumulative Roll Bonding in the System Al-Cu

Christian W. Schmidt *, Patrick Knödler, Heinz Werner Höppel and Mathias Göken

Department of Materials Science and Engineering, Institute I: General Material Properties, Friedrich-Alexander-Universität Erlangen-Nürnberg, Martensstr. 5, Erlangen 91058, Germany; E-Mails: patrick.knoedler@ww.stud.uni-erlangen.de (P.K.); hoeppel@ww.uni-erlangen.de (H.W.H.); goeken@ww.uni-erlangen.de (M.G.)

* Author to whom correspondence should be addressed;
E-Mail: christian.schmidt@ww.uni-erlangen.de; Tel.: +49-9131-8525449; Fax: +49-9131-8527504.

Received: 29 September 2011; in revised form: 11 October 2011 / Accepted: 31 October 2011 / Published: 7 November 2011

Abstract: The formation of alloys by particle reinforcement during accumulative roll bonding (ARB), and subsequent annealing, is introduced on the basis of the binary alloy system Al-Cu, where strength and electrical conductivity are examined in different microstructural states. An ultimate tensile strength (UTS) of 430 MPa for Al with 1.4 vol.% Cu was reached after three ARB cycles, which almost equals UTS of the commercially available Al-Cu alloy AA2017A with a similar copper content. Regarding electrical conductivity, the UFG structure had no significant influence. Alloying of aluminum with copper leads to a linear decrease in conductivity of 0.78 μΩ·cm/at.% following the Nordheim rule. On the copper-rich side, alloying with aluminum leads to a slight strengthening, but drastically reduces conductivity. A linear decrease of electrical conductivity of 1.19 μΩ·cm/at.% was obtained.

Keywords: accumulative roll bonding (ARB); particle reinforcement; ultrafine-grained microstructure; alloying; strength; electrical conductivity

---

1. Introduction

The accumulative roll bonding (ARB) process is a method of severe plastic deformation for sheet production and has been studied extensively regarding the evolution of microstructure and mechanical properties [1–3]. Besides the formation of an ultrafine-grained microstructure, this process offers a

high potential for tailoring properties of ultrafine-grained materials [4,5]. In this respect particle reinforcement is of special interest because it allows a high freedom in designing different spatial distributions of reinforcements [6]. It has been demonstrated that strengthening with low volume fractions of ceramic nanoparticles [7], as well as with high volume fractions of larger ceramic particles [8], is possible. Furthermore TiH_2 blowing agent particles were introduced in aluminum by this process for subsequent production of metallic foams [9]. Alloying with this process, by incorporation of metallic particles and subsequent solution annealing, has not been studied so far. A summary of applications of particle reinforcements and the achieved benefits is given in Table 1.

Table 1. Review of published applications of particle reinforcement during accumulative roll bonding (ARB).

Particle Type	Sheet	Examples Particle	Volume Fraction	Benefit	
Ceramic particles	AA1050 AA1050A AA1100 pure Cu	SiC B_4C Al_2O_3	0.06 to 15%	• Metal matrix composite formation	[5,8,10–12]
Ceramic nanoparticles	AA1050A	Al_2O_3, SiC, ZrO_2, SnO_2	0.1%	• Acceleration of microstructural evolution and strengthening	[6,7]
	AA6060	SiO_2	12% [a]	• Enhancement of bond strength	[13]
Metal hydride particles	AA1050	TiH_2	0.4% [b]	• Foam precursor material	[9]
Metallic particles	AA1050A, OFHC-Cu	Cu Al	0.3% to 3.9%	• Alloy formation	This work

[a] calculated from description in mg/mm^2; [b] calculated from description in wt.%.

In the present work the possibility of alloy formation by accumulative roll bonding with particle reinforcement is demonstrated for the binary system Al-Cu, which is well studied and shows solubility to different extents at both sides of the phase diagram. Copper and aluminum are the two most important materials for applications as conductors as they have a high conductivity at moderate cost. Copper is the most frequently used conductor material, while aluminum comes into play when density or material costs become an important issue. In many applications in modern electrical engineering, due to the trend towards miniaturization, the strength of conductor materials is continuously gaining importance. Therefore strength and electrical conductivity are evaluated in this work in different states of processing related to different microstructural states of the materials.

2. Results and Discussion

2.1. Materials Processing

Sheets of aluminum of commercial purity ≥99.5% (equal to AA1050A) and OFHC-Cu, were used as base materials for alloying with the other element in the form of metallic particles in this study. During each of six accumulative roll bonding cycles, a constant volume of particles was applied to the

respective sheet surfaces by air gun spraying from aqueous suspension as described in [6], so that a volume fraction of between 0.3% and 2.9% was achieved with copper particles in aluminum base material and volume fractions between 3.0% and 3.9% were achieved with aluminum particles in copper base material. Before roll bonding, the materials were heated to 125 °C for 300 s in order to evaporate the water from the particle suspension. As this method of inserting the same amount of particles in consecutive ARB cycles leads to a heterogeneous distribution of particles over sheet thickness [6], three further ARB cycles were added without particle addition to improve homogeneity of particle distribution in sheet thickness. This state is denoted as PS for particle strengthened (see Figures 1a (aluminum based materials), and 2a,b (copper based materials)).

Figure 1. Copper particle reinforced ultrafine-grained aluminum after nine ARB cycles in (**a**) optical micrograph showing distribution of copper particles in aluminum and (**c**) transmission electron micrograph showing copper particles and local precipitation and structure refinement in their vicinity; (**b**) optical micrograph in the PS + annealed state showing the complete dissolution of copper particles and Kirkendall porosity; (**d**) TEM of AA2017A after four ARB cycles. Please note: RD indicates rolling direction.

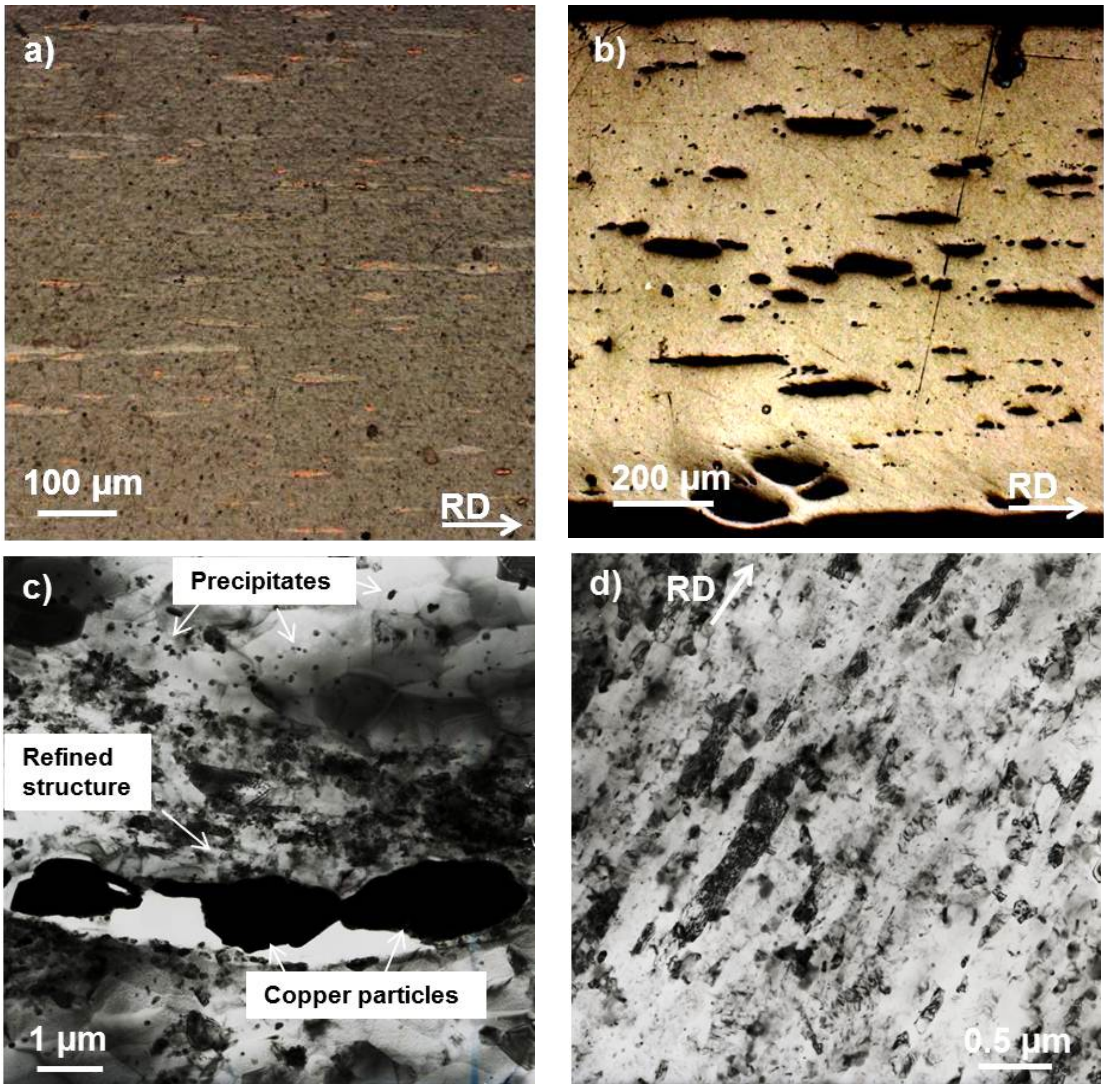

Figure 2. (**a**) Aluminum particle strengthened OFHC-Cu in optical microscope and (**b**) detail of the last bond plane. TEM microstructure of (**c**) OFHC-Cu after three ARB cycles and (**d**) OFHC-Cu alloyed with 3.8 vol.% aluminum after three ARB cycles.

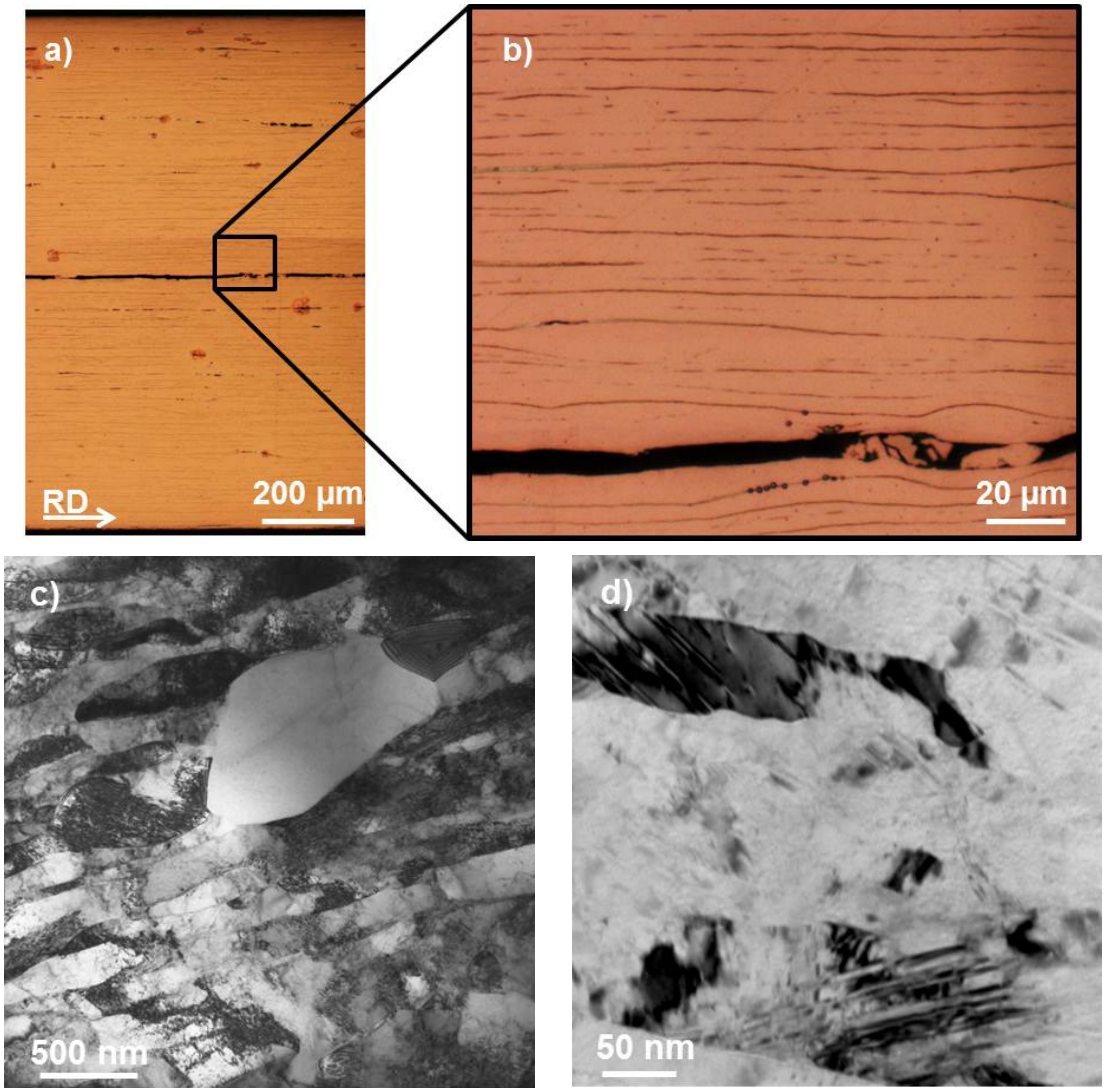

After ARB processing the samples were annealed at 530 °C for 4 h to fully dissolve the respective metallic particles in the sheets, as proven by OM (see Figure 1b) and SEM. This second microstructural state is called PS + annealed. The annealed materials were conventionally ARB processed including heating at 125 °C for 300 s again for three cycles to restore an ultrafine-grained microstructure in the alloyed samples which had been destroyed during solutionizing. This third state is denoted as PS + annealed + N3. The designation of materials is summarized in Table 2. Further deformation would have been beneficial for strength but was disregarded due to increasing edge cracking of the sheets. Additionally for reference on the aluminum-rich side, aluminum-copper alloy AA2017A was investigated because of a comparable copper content (3.5 wt.% to 4.5 wt.% is equivalent to 1.1 vol.% to 1.4 vol.%) and relatively low content of other alloying elements (see composition in Table 3). The commercial reference alloy AA2017A was ARB processed without any particle addition at room temperature to different grades of deformation.

Table 2. Designation of materials, their processing history and microstructural states.

Designation	Starting material and processing history	Microstructural state
PS	Recrystallized AA1050A + 6 ARB cycles with particle application + 3 ARB cycles without particle application	particle reinforced pure metal with UFG structure
PS + annealed	PS + solutionizing (530 °C/4 h)	binary alloy with CG structure
PS + annealed + N3	PS + annealed + 3 ARB cycles without particle application	binary alloy with UFG structure

Table 3. Composition of the applied sheet materials (max. values).

wt.%	**Si**	**Fe**	**Cu**	**Mn**	**Mg**	**Zn**	**Ti**	**Cr**	**Ni**	**others**	**Al**
AA1050A	0.25	0.40	0.05	0.05	0.05	0.07	0.05	-	-	0.03	balance
AA2017A	0.80	0.70	4.50	1.00	1.00	0.25	-	0.10	0.25	0.05	balance
ppm	**S**	**Fe**	**Ni**	**O**	**P**						**Cu**
OFHC-Cu	15	10	10	5	3						balance

2.2. Aluminum Reinforced with Copper

In the recrystallized state, the commercially pure AA1050A exhibits very low yield strength (YS) of around 40 MPa and ultimate tensile strength (UTS) of around 75 MPa. By ARB processing up to nine cycles YS and UTS can be increased to around 135 and 160 MPa respectively as shown in Figure 3. In this context it has to be mentioned, that the strength in the UFG state strongly depends on the amount and composition of impurities.

Figure 3. Stress-strain data of AA1050A reinforced with different selected amounts of copper particles in different microstructural states: Particle strengthened after nine ARB cycles (PS), solution annealed in a further process step (PS + annealed) and after further three ARB cycles (PS + annealed + N3).

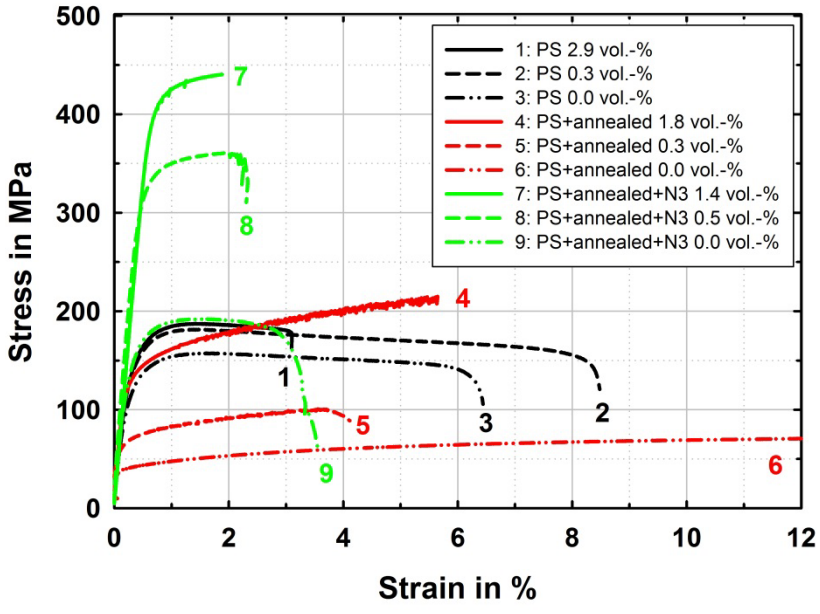

When copper particles are applied during the ARB process, the strength can be further improved by approximately 25 MPa. This can be understood by additional plastic deformation around the particles, which are harder than the matrix, and therewith locally enhanced grain refinement [6,14]. Among the volume fractions of copper particles applied here from 0.3% to 2.9%, the difference in strength is only about 5 MPa. This confirms that already small amounts of particles (here 0.3%) are sufficient for additional strengthening [6,7] and a further increase in volume fraction hardly influences strength. Microstructural investigations by TEM (see Figure 2c) show that an ultrafine-grained microstructure in the particle-reinforced ultrafine-grained state is achieved and that especially in the vicinity of copper particles there are regions of further refined grains as well as precipitates. These precipitates must have formed during the mild heating step of the sheets during each ARB cycle. It has to be mentioned that both, precipitates and further refined areas are solely local phenomena around the introduced copper particles. It can therefore be concluded that the strengthening in the ultrafine-grained state due to particle reinforcement originates from these local phenomena as previously described for other reinforcing particles [6,7]. Additionally precipitation hardening further strengthens the material. Therefore strengthening by metallic copper particles is greater than applying ceramic particles.

After solutionizing, the materials in the PS+annealed state with CG microstructure show the typical behavior of pronounced strain hardening with a decided effect of copper content on strength. While the yield strength of these solid solution strengthened CG samples is clearly lower than in the ultrafine-grained PS state, the ultimate tensile strength of the CG samples even exceeds those of the UFG samples in case of high copper content. On the other hand, the annealed samples exhibit a long strain hardening domain and predominantly fail during strain hardening due to bond plane defects related to the ARB process. In contrast, the samples in ultrafine-grained PS state show reduced uniform elongation of 1.3% to 1.5%.

After further ARB processing for three cycles, an ultrafine-grained microstructure is restored in the PS + annealed + N3 samples and very high strength in the region of 350 to 430 MPa is reached depending on the copper content while ductility is reduced. Elongation to failure ranges between 2% and 3%, while for high copper contents above 1.8 vol.% all the specimens fractured without considerable plastic deformation. Though the uniform elongation is prolonged compared to the particle strengthened and pure ultrafine-grained materials, no further strain can be applied after reaching that limit. Again here in this PS + annealed + N3 state, there is a dependence of strength on the copper content. Especially the material with the lowest copper content shows a clearly lower strength than the materials with higher content of solute copper. The influence of copper content on strength in this PS + annealed + N3 state must be related on the one hand to solid solution strengthening and on the other hand to the decrease of saturation grain size by higher solute content.

The high strength after three ARB cycles in the alloyed materials should be compared to a commercial AlCu alloy from the AA2xxx-series for judging the comparability of mechanical properties of the samples produced by alloying through ARB processing and subsequent annealing. After three ARB cycles the AA2017A reaches slightly higher strength (UTS = 474 MPa) than the binary alloyed samples with comparable copper content after the same degree of deformation (UTS = 413 to 442 MPa). The higher strength of the commercial alloy compared to the binary alloy might be related to further minor alloying elements like magnesium, manganese and silicon. Furthermore it can be seen from the tensile tests on AA2017A after five ARB cycles (Figure 4) that

further strengthening potential is still available in Al-Cu alloys. An ultimate tensile strength of 570 MPa can be reached after five ARB cycles, before further deformation leads to drastic reduction of ductility and cracking of the material during processing. This was already observed for Al-Cu alloys during equal channel angular pressing (ECAP), where backpressure and/or elevated temperatures were necessary to avoid cracking in AA2024 [15] and AA2124 [16]. However, here by ARB processing at room temperature approximately the same strength of AA2017 is reached before damage of the material occurs by further deformation as by ECAP with backpressure at room temperature [17]. The very high strength achieved by severe plastic deformation of Al-Cu alloys demonstrates their high potential for lightweight applications.

Figure 4. Selected stress-strain data of the commercial alloy AA2017A after ARB processing to different ARB cycles N1 to N6 and reference state W (solutionized).

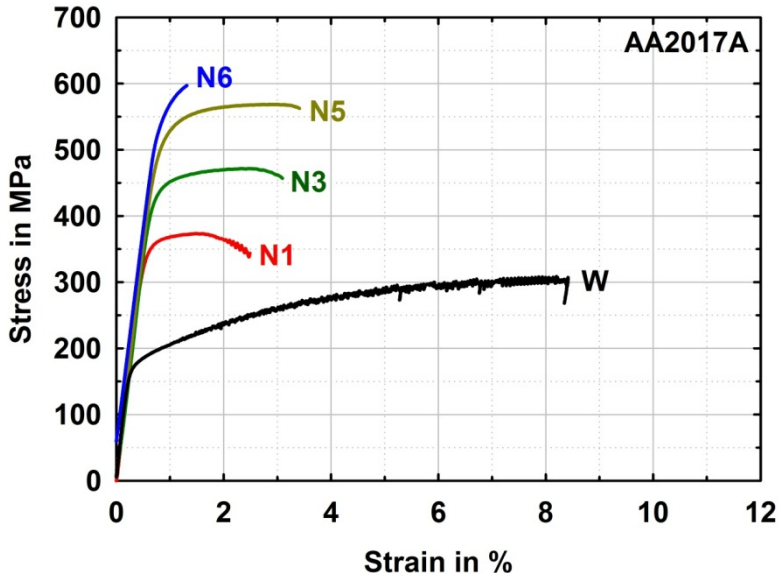

While microstructural defects like a high dislocation density, a high volumetric share of grain boundaries as well as precipitates and solute atoms are strengthening a material, any such microstructural defect weakens—to different extents—the electrical conductivity. In the produced materials, considerable differences in strength are shown; high strengths are achieved by different strengthening mechanisms and these different mechanisms incur a strong influence on conductivity. Therefore there is always a conflict of goals between high defect density causing high strength and low defect density causing high electrical conductivity. Hence, for any specific application balance between strength and conductivity has to be achieved.

The electrical conductivity of the produced aluminum materials in the different microstructural states is depicted in Figure 5. It can be seen that the ultrafine-grained microstructure slightly reduces the conductivity by less than $1 \times 10^6/\Omega m$, while the reinforcement with copper particles of between 0.3 vol.% and 2.9 vol.% has no significant effect on conductivity. In the PS + annealed state, after solution heat treatment, there is a clear effect of the copper content. As the formed solid solution is in an unordered state, Nordheim rule [18] can be applied. This rule states that the loss in conductivity is proportional to $x(1 - x)$, where x is the mole fraction of solute atom in a disordered state. For low contents this rule results in a linear relationship to the mole fraction. The Nordheim coefficient is

measured to be 0.78 μΩ·cm/at.%, which is very close to the 0.80 μΩ·cm/at.% published by Kedves *et al.* [19]. As mole fraction is also approximately linear to volume fraction for low contents this linear relationship predicted by the Nordheim rule is still linear in the illustration in Figure 5.

Figure 5. Electrical conductivity of the aluminum based materials in different microstructural states depending on the copper content. Dashed lines symbolize solubility of Cu in Al at 530 °C (vertical) and conductivity of AA1050A in CG state (horizontal).

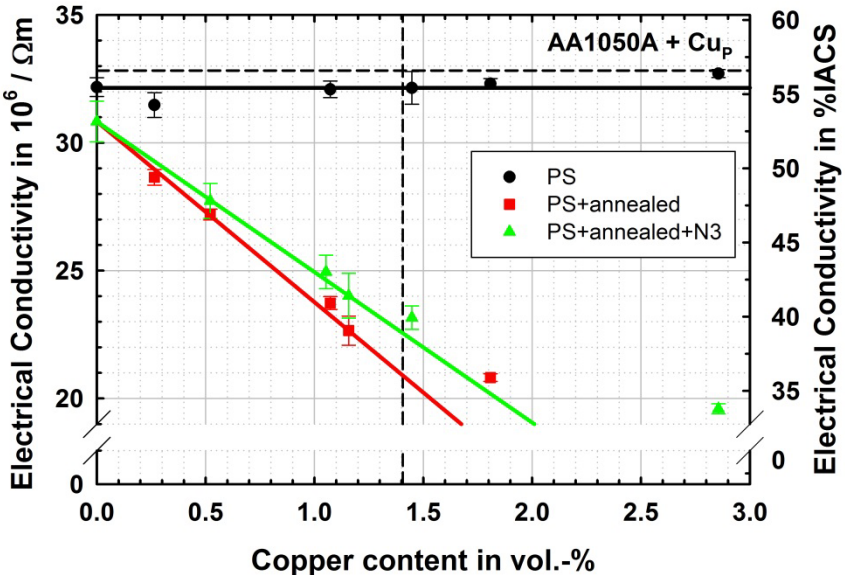

For the ultrafine-grained alloyed materials (PS + annealed + N3) also a linear drop of conductivity with increasing copper content is observed, although the drop is less steep in this case. One would normally expect a parallel linear description of the measurement due to Nordheim rule and the disordered solute content and furthermore a little lower conductivities due to the ultrafine-grained microstructure. These effects are superimposed by the onset of precipitation caused by the mild warming during ARB processing. As during the second ARB processing after solution heat treatment, the materials are pre-heated for 5 min at 125 °C in each of the three cycles and because the solubility of copper in aluminum is very limited in this temperature region, there is precipitation occurring. With ongoing precipitation, the solute content is inherently reduced leading to relatively higher conductivities while the precipitates themselves should also deteriorate conductivity but to a lesser extent than the solutes. This can also be seen by the samples in the PS + annealed and the PS + annealed + N3 state at higher copper contents above the solubility. Here although a decrease of conductivity with increasing copper content is found, the measured values are above the extrapolation of the Nordheim rule lines, indicating that the gradient of the decrease is reduced as the solid solution is saturated and copper can be exclusively located in precipitates.

2.3. Copper Reinforced with Aluminum

Aluminum reinforced copper is a very interesting field of research as the aluminum content in copper strongly determines the stacking fault energy [20,21] and, therewith, the deformation mode changes from dislocation slip in pure copper to a coexistence of dislocation slip and deformation

twinning towards pure deformation twinning [22]. Besides the stacking fault energy, which is directly influenced by the aluminum content, the Zener-Hollomon parameter [23], which is governed by the deformation strain rate and temperature for a given material, is of high importance to the predominant deformation mechanism [22]. In this work pure copper and copper with an aluminum content between three and four volumetric percent deformed under a Zener-Hollomon parameter of ln Z = 32.9 are examined. Therefore according to previous studies reviewed by Zhang *et al.* [22], pure copper as well as all prepared alloys are in the area of competing deformation mechanisms, while in the pure copper sample dislocation slip should clearly dominate and in the alloyed samples with increasing aluminum content twinning should gain more and more importance. This prediction is verified by TEM investigations (see Figure 2c,d).

The mechanical properties of the produced copper materials in the particle strengthened ultrafine-grained PS (see Figure 2a,b), the PS + annealed, and the PS + annealed + N3 (see Figure 2c,d) state are displayed in Figure 6. The ultrafine-grained pure copper samples reach UTS between 400 and 450 MPa, which is typically achieved by accumulative roll bonding on pure copper [2,24–27]. Aluminum particle reinforcement leads to a slight strengthening, which may be based on local straining and onset of dissolution of aluminum in copper and therewith slight solid solution strengthening due to processing at 125 °C. After solution heat-treatment the strength clearly increased compared to the CG reference material due to complete dissolution of aluminum particles and therewith a clear effect of solid solution strengthening. In the narrow range of the aluminum content tested here, the effect of different aluminum contents is not becoming clearly resolved in the measurements. After further ARB treatment, a considerable difference in strength is observed between pure copper and alloyed copper with increasing aluminum content, while also the amount of aluminum has a strong effect even in the narrow regime tested here.

Figure 6. Stress-strain data of OFHC-Cu reinforced with different selected amounts of aluminum particles in different microstructural states. Particle strengthened after nine ARB cycles (PS), solution annealed in a further process step (PS + annealed) and after a further three ARB cycles (PS + annealed + N3).

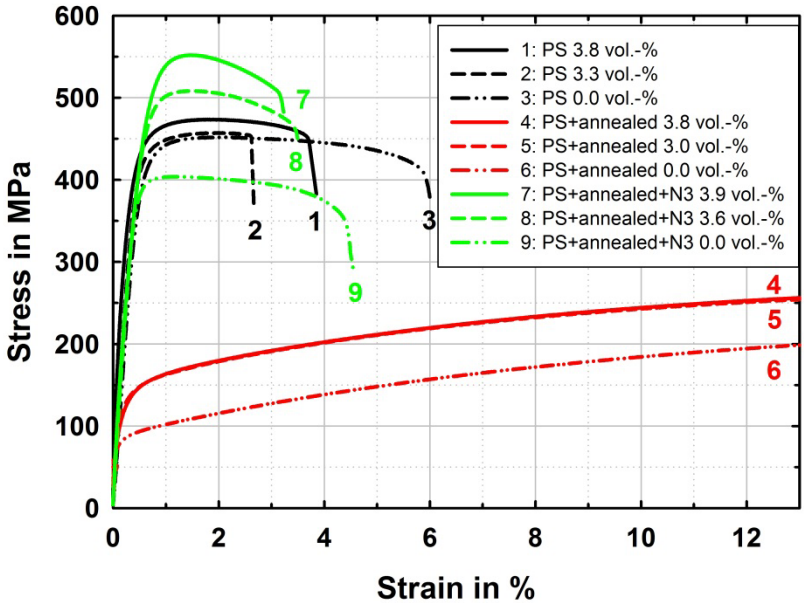

The electrical conductivity behaves as expected from the measurements on copper reinforced aluminum. The ultrafine-grained microstructure as well as particle content does not significantly decrease conductivity. The influence of grain size on conductivity in copper is discussed by Takata *et al.* [25] and Champion *et al.* [28] differently. While Takata *et al.* [25] show that until the grain size is reduced below approximately 300 nm the decrease in conductivity in copper due to grain boundaries is very limited, Champion *et al.* [28] theoretically derived an equation for the resistivity of copper due to grain boundaries which suggests an immense drop to about 5% IACS at this grain size. An exception from this rule is given by highly twinned copper as produced by Lu *et al.* [29], which results in a high strength of about 1 GPa at nearly unreduced conductivity. The results of conductivity in the different microstructural states depending on the aluminum content are shown in Figure 7.

Figure 7. Electrical conductivity of the copper based materials in different microstructural states depending on the aluminum content. The dashed line symbolizes conductivity of OFHC-Cu in CG state.

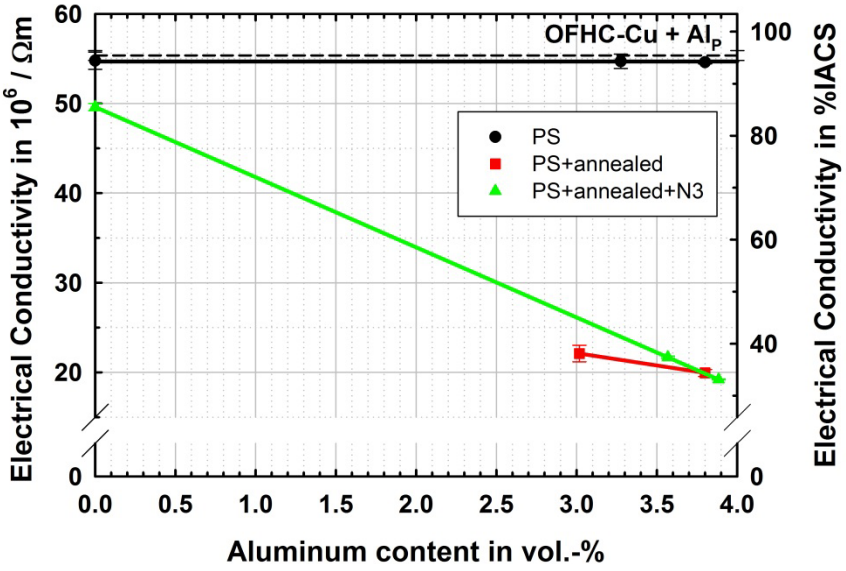

In accordance with Takata *et al.* [25], the drop of conductivity for ultrafine-grained pure copper is very small and within the error of measurement. Also with addition of aluminum particles, no significant drop in conductivity is observed. In the alloyed samples produced by particle reinforced ARB and subsequent annealing conductivity is drastically reduced and the amount of reduction seems to show a linear relation to the aluminum content as proposed by the Nordheim rule [18]. Here the Nordheim coefficient can be determined to be 1.19 μΩ·cm/at.% which is very close to 1.25 μΩ·cm/at.%, as determined by Linde [30]. In the PS + annealed + N3 state the conductivity is quite close to the PS + annealed state for comparable aluminum contents.

2.4. Simultaneous Consideration of Electrical Conductivity and Strength

As it has been shown in the Al-Cu system, strength and electrical conductivity are strongly affected by different microstructural states and alloying contents. It becomes obvious that both properties cannot be improved simultaneously. Therefore a balance between both has to be found for practical use. For this reason Figure 8 compares yield strength to electrical conductivity of the produced

materials in their different states. The trends in all series of materials have been discussed before, but here it is conclusively shown that on the aluminum side (Figure 8a), the ultrafine-grained alloyed state is the most promising due to the high strength and reasonable conductivity. Further potential for improvement of strength is shown by the commercial reference alloy AA2017A which shows a further increase of yield strength of about 150 MPa is possible with higher deformations and only moderate further loss of conductivity.

On the copper side (Figure 8b), it is demonstrated that in this binary system slight strengthening can be achieved by alloying but the loss in conductivity is immense. Nevertheless introduction of an ultrafine-grained microstructure into pure copper seems very promising for applications, as in this case, yield strength is increased by a factor of 4 compared to the CG material, while conductivity is not significantly reduced. An overwhelming combination of properties seems to be possible in this respect with nano-twinned copper as reported by Lu *et al.* [29], where strength is very high and conductivity is still close to that of pure, conventionally grained copper.

Figure 8. Yield strength and electrical conductivity of (**a**) aluminum based materials in different microstructural states; (**b**) copper based materials in different microstructural states. Please note: Unreinforced materials are labeled with a circle around the symbol.

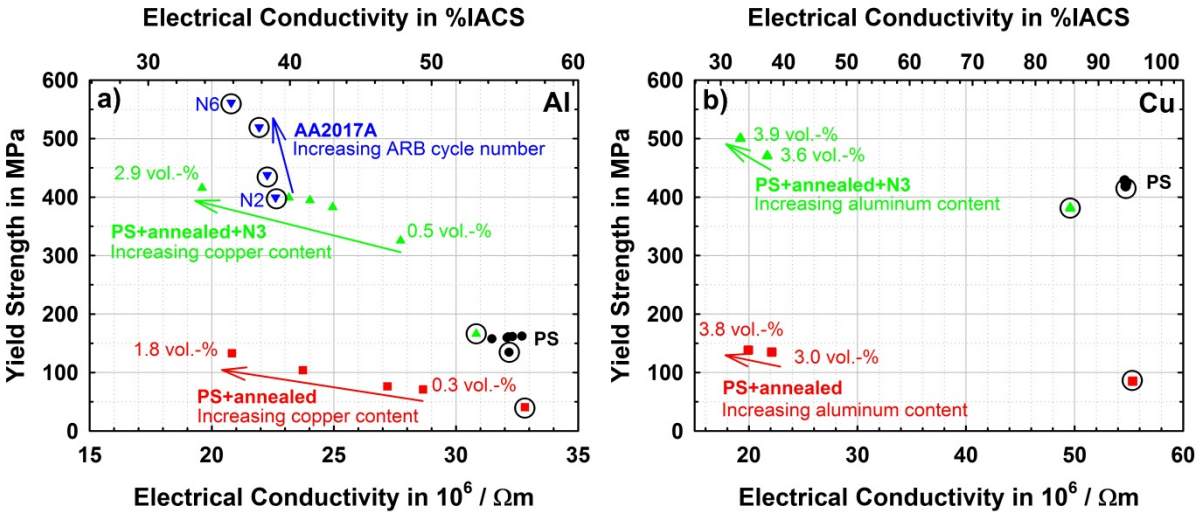

3. Experimental Section

Accumulative roll bonding was performed using two sheets with a size of 300 mm × 100 mm and a thickness of 1 mm. Before ARB processing the AA1050A sheet material was recrystallized for 1 h at 500 °C and quenched in water, OFHC-Cu was applied in the recrystallized state as delivered and AA2017A was solutionized at 530 °C for 30 min. Surface treatment consisting of acetone cleaning and wire brushing was performed to clean the surfaces and facilitate bonding during the following roll bonding step. Between surface treatment and roll bonding with a reduction of 50% the respective metallic particles were inserted between the sheets. Aluminum particles (ECKA Aluminiumgrieß AS < 10 µm MEP 105, Mepura Metallpulver Gesellschaft mbH, Ranshofen, Austria) with a median particle size of 4.4 µm and a purity >99.5% and copper particles (ECKA MicroTronic120, ECKA Granules Germany GmbH, Fürth, Germany) with a median particle size between 0.6 and 1.3 µm and a

purity >99.4% are used as second phase introduced during ARB processing. The particles are dispersed in aqueous suspension with a mass concentration of 33% without stabilizer.

Mechanical characterization of the samples was done by uniaxial tensile testing at room temperature at a strain rate of 10^{-3} s^{-1} using an Instron 4505 universal testing machine. Measurements of electrical conductivity were performed on wires with a rectangular cross section of approximately 1 mm^2 cut from the sheets applying the 4-wire sensing method over a length of 7 cm. Electrical conductivity is displayed in $10^6/\Omega m$ as well as in %IACS (electrical conductivity relative to the international annealed copper standard of 58 × $10^6/\Omega m$). Microstructural characterization was performed in transmission electron microscope (TEM) Philips CM-200 and optical microscope (OM) Zeiss Axio Imager.M1.

Calculation of the Zener-Hollomon parameter was executed taking the activation energy for grain boundary self-diffusion in copper of 72.5 kJ mol^{-1} [31], temperature of 20 °C and deformation strain rate of 23.5 s^{-1} calculated according to [32] with working roll diameter d = 32.5 mm, reduction = 50%, roll surface velocity = 8 m/min.

4. Conclusions

In this work a new application for particle reinforcement during the accumulative roll bonding (ARB) process was demonstrated by alloying and annealing of metallic particle reinforced sheet metals. The method was demonstrated on both sides of the binary alloy system Al-Cu, regarding strength and electrical conductivity as the two key properties of materials of this system. It could be shown that alloying by ARB and subsequent annealing leads to comparable material properties to those of commercial alloys with a similar composition. The high potential of aluminum-copper alloys with regard to lightweight constructions and electrical conductivity problems, where considerable strength is requested was also demonstrated; ultrafine-grained copper exhibits great promise for such applications.

This method opens up a wide field of alloying possibilities which are added to the various options for producing tailored ultrafine-grained sheet materials by this process, while the future benefit of this method will be the freedom of design concerning composition and spatial distribution of the reinforcement in any form. Therefore this new method should not only be of interest for tailored applications, but also for scientific purposes, when local alloy formation is being investigated.

Acknowledgments

The authors gratefully acknowledge the funding of the German Research Council (DFG), which, within the framework of its “Excellence Initiative” supports the Cluster of Excellence “Engineering of Advanced Materials” at the University of Erlangen-Nürnberg. Additionally the authors want to thank ECKA Granules Germany GmbH and Mepura Metallpulvergesellschaft mbH for the kind supply of metal powder samples.

References

1. Saito, Y.; Tsuji, N.; Utsunomiya, H.; Sakai, T.; Hong, R.G. Ultra-fine grained bulk aluminum produced by accumulative roll-bonding (ARB) process. *Scr. Mater.* **1998**, *39*, 1221–1227.
2. Tsuji, N.; Saito, Y.; Lee, S.-H.; Minamino, Y. ARB (accumulative roll bonding) and other new techniques to produce bulk ultrafine grained materials. *Adv. Eng. Mater.* **2003**, *5*, 338–344.
3. Höppel, H.W.; May, J.; Göken, M. Enhanced strength and ductility in ultrafine-grained aluminium produced by accumulative roll bonding. *Adv. Eng. Mater.* **2004**, *6*, 781–784.
4. Göken, M.; Höppel, H.W. Tailoring nanostructured, graded, and particle-reinforced Al laminates by accumulative roll bonding. *Adv. Mater.* **2011**, *23*, 2663–2668.
5. Hausöl, T.; Maier, V.; Schmidt, C.W.; Winkler, M.; Höppel, H.W.; Göken, M. Tailoring materials properties by accumulative roll bonding. *Adv. Eng. Mater.* **2010**, *12*, 740–746.
6. Schmidt, C.W.; Knieke, C.; Maier, V.; Höppel, H.W.; Peukert, W.; Göken, M. Accelerated grain refinement during accumulative roll bonding by nanoparticle reinforcement. *Scr. Mater.* **2011**, *64*, 245–248.
7. Schmidt, C.W.; Knieke, C.; Maier, V.; Höppel, H.W.; Peukert, W.; Göken, M. Influence of nanoparticle reinforcement on the mechanical reinforcement of ultrafine-grained aluminium produced by ARB. *Mater. Sci. Forum* **2011**, *667–669*, 725–730.
8. Jamaati, R.; Toroghinejad, M.R. Manufacturing of high-strength aluminum/alumina composite by accumulative roll bonding. *Mater. Sci. Eng. A* **2010**, *527*, 4146–4151.
9. Kitazono, K.; Sato, E.; Kuribayashi, K. Novel manufacturing process of closed-cell aluminium foam bay accumulative roll bonding. *Scr. Mater.* **2004**, *50*, 495–498.
10. Alizadeh, M.; Paydar, M.H. Fabrication of nanostructure Al/SiC_P composite by accumulative roll-bonding (ARB) process. *J. Alloy. Compd.* **2010**, *492*, 231–235.
11. Alizadeh, M. Comparison of nanostructured Al/B_4C composite produced by ARB and Al/B_4C composite produced by RRB process. *Mater. Sci. Eng. A* **2010**, *528*, 578–582.
12. Jamaati, R.; Toroghinejad, M.R. Application of ARB process for manufacturing high-strength, finely dispersed and highly uniform Cu/Al_2O_3 composite. *Mater. Sci. Eng. A* **2010**, *527*, 7430–7435.
13. Lu, C.; Tieu, K.; Wexler, D. Significant enhancement of bond strength in the accumulative roll bonding process using nano-sized SiO_2 particles. *J. Mater. Process. Technol.* **2009**, *209*, 4830–4834.
14. Humphreys, F.J.; Prangnell, P.B.; Bowen, J.R.; Gholinia, A.; Harris, C. Developing stable fine-grain microstructures by large strain deformation. *Philos. Trans. R. Soci. A* **1999**, *357*, 1663–1681.
15. Kim, W.J.; Chung, C.S.; Ma, D.S.; Hong, S.I.; Kim, H.K. Optimization of strength and ductility of 2024 Al by equal channel angular pressing (ECAP) and post-ECAP aging. *Scr. Mater.* **2003**, *49*, 333–338.
16. Lapovok, R.; Loader, C.; Dalla Torre, F.H.; Semiatin, S.L. Microstructure evolution and fatigue behavior of 2124 aluminum processed by ECAE with back pressure. *Mater. Sci. Eng. A* **2006**, *425*, 36–46.
17. Hockauf, M.; Meyer, L.W.; Krüger, L. Combining equal-channel angular extrusion (ECAE) and heat treatment for achieving high strength and moderate ductility in an Al-Cu alloy. *Mater. Sci. Forum* **2008**, *584–586*, 685–690.

18. Nordheim, L. Zur Elektronentheorie der Metalle. I. *Ann. Phys.* **1931**, *401*, 607–640.
19. Kedves, F.J.; Gergely, L.; Hordós, M.; Kovács-Cseténvi, E. Temperature dependence of impurity resistivity in dilute Al-based Ti, V, Fe, Cu, Zn alloys between 78 and 930 K. *Phys. Status Solidi A* **1972**, *14*, 561–564.
20. Johari, O.; Thomas, G. Substructures in explosively deformed Cu and Cu-Al alloys. *Acta Metall.* **1964**, *12*, 1153–1159.
21. Rohatgi, A.; Vecchio, K.S.; Gray, G.T., III. The influence of stacking fault energy on the mechanical behavior of Cu and Cu-Al alloys: Deformation twinning, work hardening, and dynamic recovery. *Metall. Mater. Trans. A* **2001**, *32A*, 135–145.
22. Zhang, Y.; Tao, N.R.; Lu, K. Effects of stacking fault energy, strain rate and temperature on microstructure and strength of nanostructured Cu-Al alloys subjected to plastic deformation. *Acta Mater.* **2011**, *59*, 6048–6058.
23. Zener, C.; Hollomon, J.H. Effect of strain rate upon plastic flow of steel. *J. Appl. Phys.* **1944**, *15*, 22–32.
24. Shaarbaf, M.; Toroghinejad, M.R. Nano-grained copper strip produced by accumulative roll bonding process. *Mater. Sci. Eng. A* **2008**, *473*, 28–33.
25. Takata, N.; Lee, S.-H.; Tsuji, N. Ultrafine grained copper alloy sheets having both high strength and high electric conductivity. *Mater. Lett.* **2009**, *63*, 1757–1760.
26. Han, S.Z.; Lim, C.; Kim, C.J.; Kim, S. Mechanical properties of SPD (severe plastic deformation) processed copper. *Mater. Sci. Forum* **2005**, *475–479*, 3497–3500.
27. Jang, Y.H.; Kim, S.S.; Han, S.Z.; Lim, C.Y.; Kim, C.J.; Goto, M. Effect of trace phosphorous on tensile behavior of accumulative roll bonded oxygen-free copper. *Scr. Mater.* **2005**, *52*, 21–24.
28. Champion, Y.; Bréchet, Y. Effect of grain size reduction and geometrical confinement in fine grained copper: Potential applications as material for reversible electrical contacts. *Adv. Eng. Mater.* **2010**, *12*, 798–802.
29. Lu, L.; Shen, Y.; Chen, X.; Qian, L.; Lu, K. Ultrahigh strength and high electrical conductivity in copper. *Science* **2004**, *304*, 422–426.
30. Linde, J.O. An experimental study of the resistivity–concentration dependence of alloys. *Helv. Phys. Acta* **1968**, *41*, 1007–1015.
31. Mishra, A.; Kad, B.K.; Gregori, F.; Meyers, M.A. Microstructural evolution in copper subjected to severe plastic deformation: Experiments and analysis. *Acta Mater.* **2007**, *55*, 13–28.
32. Kojima, S.; Yokoyama, A.; Komatsu, M.; Kiritani, M. High-speed deformation of aluminium by cold rolling. *Mater. Sci. Eng. A* **2003**, *350*, 81–85.